INTERNATIONAL JOURNAL OF HYDROGEN ENERGY 47 (2022) 26901–26914

Available online at www.sciencedirect.com

ScienceDirect

journal homepage: www.elsevier.com/locate/he

Characterization of pores and microfractures in tight conglomerate reservoirs

Ziqiang Wang [a,b,c], Hongkui Ge [a], Wei Zhou [b], Yun Wei [b], Bei Wang [b], Sai Liu [b], Hao Zhou [b], Shuheng Du [d,e,*]

[a] China University of Petroleum, Beijing, 102249, China

[b] Research Institute of Exploration and Development, Xinjiang Oilfield Company, Karamay 834000, China

[c] Xinjiang Key Laboratory of Shale Oil Exploration and Development, Karamay, 834000, China

[d] State Key Laboratory of Nonlinear Mechanics, Institute of Mechanics, Chinese Academy of Sciences, Beijing, 100190, China

[e] School of Engineering Science, University of Chinese Academy of Sciences, Beijing, 100049, China

HIGHLIGHTS

- Pores and microfractures extractions by machine learning are used.
- Microfractures contribute more to energy storage and seepage than pores.
- Stress, cementation and corrosion control the complex geometric properties.
- Pores and microfractures are geometrically heterogeneous.
- The development of microfractures and pores are linked closely.

GRAPHICAL ABSTRACT

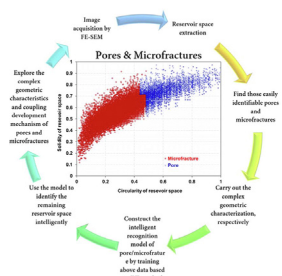

ARTICLE INFO

Article history:
Received 29 March 2022
Received in revised form
16 May 2022
Accepted 5 June 2022
Available online 11 July 2022

Keywords:
Mahu sag
Tight conglomerate

ABSTRACT

This study aimed to carry out the data-driven evaluation of pores and microfractures in tight conglomerate reservoirs combining machine learning and complex geometric analysis, then investigate the internal control factors of reservoir damage.

Results show that for the Upper Wuerhe formation of Mahu sag in Xinjiang of China, the average contribution rate of microfractures to fluid storage and seepage is 7.1 times that of pores, and microfractures dominate in fluid storage and seepage. Besides, the average contact probability between microfractures and fluids is 3.0 times that of pores. Compared with microfractures, pores are more conducive to form a homogeneous distribution of seepage flow and expand the sweep efficiency. On the contrary, microfracture is the dominant factor to aggravate the heterogeneity of seepage.

* *Corresponding author*. State Key Laboratory of Nonlinear Mechanics, Institute of Mechanics, Chinese Academy of Sciences, Beijing, 100190, China.

E-mail address: dushuheng@imech.ac.cn (S. Du).

https://doi.org/10.1016/j.ijhydene.2022.06.037

Pore
Microfracture
Characterization
Machine learning

The conclusions will provide crucial theoretical support and practical basis for the effective exploitation of tight conglomerate oil.

Introduction

In the third decade of the 21st century, fossil energy still plays a key role in the development and progress of human society [1–5]. Scholars have carried out many useful scientific studies on the exploration [6–10], development [11–16] and effective utilization [17–21] of the above types of fossil energy. With the continuous advancement of unconventional energy exploration and development, tight oil has gradually become an irreplaceable part of global fossil energy [22,23]. As the largest conglomerate oil field discovered so far in the world, Mahu oilfield in Xinjiang has become a crucial replacement area for increasing reserves and production of unconventional energy in China. The tight conglomerate reservoir represented by the Upper Wuerhe formation in Mahu sag has typical characteristics of mixed rock and mineral, diversified storage and seepage space, obvious reservoir damage and high difficulty of exploitation [24–29]. Long term research and practice have shown that how to accurately characterize the reservoir spatial characteristics of such rocks has become an important direction for the investigation on oil storage and flow mechanism, and is also a frontier scientific problem in the field of petroleum geology [30–32]. At the same time, facing the key problems such as the effective identification and development mechanism of pores and microfractures in conglomerate, there is still a lack of effective research ideas, which makes it difficult to carry out reservoir stimulation, and then seriously restricts the improvement of oil recovery, so it is urgent to conduct in-depth research.

Pores and fractures are the common places for the occurrence and flow of primary and foreign fluids in rocks, and they are important attributes of all fossil energy reservoir rocks [33–36]. For tight conglomerate reservoirs, the formation of pores and fractures depends on the accumulation and arrangement of skeleton minerals and interstitial particles. As the most important reservoir space for hydrocarbon, the development degree and structural characteristics of pores will have a decisive impact on the hydrocarbon reserves and the final upper limit of production [37–40]. At the same time, microfractures with different sizes and shapes are widely developed in the dense conglomerate, which will undoubtedly be a "double-edged sword" affecting the exploitation of hydrocarbon. For the enrichment and preservation of hydrocarbon, if the scale of microfracture extends to a certain threshold step by step, it will lead to the loss of reserves, the reduction of original hydrocarbon saturation and the decline of exploitation potential; However, for the effective exploitation of crude fossil hydrogen energy, the development of microfractures helps to form new seepage channels, so as to improve the flow performance of hydrocarbon and the final recovery degree of fluid [41–43]. In addition, the strong heterogeneity and anisotropy of microfracture development can directly affect the displacement efficiency of injection agent and is also one of the fundamental reasons for the formation of remaining oil [44–46].

Pores and fractures are two main types of reservoir space in rocks. Scholars have focused on above two types of reservoir space and carried out a set of studies on the qualitative description and quantitative computation [46–50]. For tight conglomerate, the role of pores and microfractures in the whole process of oil exploration and development is different. Pores mainly play the role of storing hydrocarbon and provide auxiliary seepage channels for hydrocarbon exploitation; On the contrary, microfractures mainly provide the core seepage channel for the efficient transportation of hydrocarbon, and also provide auxiliary space for the storage of hydrocarbon. However, if the reservoir space type of rock is mainly pore or microfracture, which accounts for a large proportion of the reservoir space type, it would dominate the reservoir and seepage process of rock at the same time, the contribution rate of pore and microfracture to reservoir and seepage can also be calculated quantitatively [51–53]. At the same time, due to the coexistence of pores and microfractures in rocks, there must be an interactive mechanism in their development, but at present, there is a lack of research in this field.

It is very necessary to extract pores and microfractures in turn and then conduct in-depth research respectively, which has indispensable quantitative scientific and engineering significance for thoroughly clarifying the enrichment and exploitation of hydrocarbon. However, according to the current research status, for the same rock, the research idea of studying its internal pores and microfractures separately and exploring the development mechanism under the background of the interaction between pores and microfractures has not been paid enough attention, which is the research direction of this study.

In view of the above research status, the noverty of this study is reflected in that pores and microfractures in unconventional hydrocarbon reservoirs are firstly extracted precisely, the average contribution rates of microfractures and pores to fluid storage and seepage are figured out and the development mechanism of the complex geometric properties of microfractures and pores are finally investigated.

Methodology

Research background

The study area located in Mahu sag, Junggar Basin, Xinjiang, China. At present, proven oil reserves are 120 million tons.

Among them, the Permian Upper Wuerhe formation is the main contributing stratum in Mahu 1 well area [24,25].

According to the logging curve characteristics of well "K205" in Mahu area (Fig. 1), the whole formation of the oilfield could be divided into two sets of strata P3W2 and P3W1 for development. Among them, P3W2 can be subdivided into P3W21 (hereinafter referred to as W2-1) and P3W2-2 (hereinafter referred to as W22), and P3W1 can be further subdivided into P3W1-1 (hereinafter referred to as W11) and P3W2-2 (hereinafter referred to as W12).

At present, the method combining horizontal well and volume fracturing is adopted for development, but the production is poor, the recoverable reserves of single well (EUR) are low (up to 29,000 tons). Preliminary research and engineering practice show that physical and chemical factors such as water sensitivity, hydration and pressure sensitivity are important mechanisms that lead to large-scale damage to the storage and seepage performance of this type of rock and inhibit the significant increase of its recovery [26,27].

From the perspective of sedimentary geology, the Upper Wuerhe formation is a set of large lakes transgressive and retrograde fan deltas, and the reservoir rock is mainly sandy conglomerate. The reservoir is mainly developed in the channel of fan delta plain and the underwater distributary channel of fan delta front [28,29]. Since there are significant differences in reservoir and seepage space in various types of conglomerate formed by complex geological processes, there should also be very obvious heterogeneity in the contribution rate of pores and microfractures to reservoir and seepage.

Technical route

The technical route is mainly reflected in Fig. 2, which fully shows the overall context of this research.

Step 1: Image acquisition by field emission scanning electron microscope (FE-SEM). We made the physical sample of conglomerate by precision wire cutting and placed it under the high-resolution FE-SEM to obtain the high-precision rock backscatter image.

Step 2: Find those easily identifiable pores and microfractures. According to the traditional definition of pores and microfractures, a series of easily identifiable pores and microfractures are selected directly by using the method of manual identification. Take them as research objects to the segmentation methods of pores and microfractures.

Step 3: Carry out the complex geometric characterization carefully. The reservoir space of rock is extracted by image processing, and two types of characterization parameters are introduced: pore (microfracture) size and geometric shape, the values of all kinds of parameters are calculated respectively. Among them, the size parameters include two types of lengths and widths. The first type of length and width indicates maximum Feret diameter (herein referred to as "pore length" and "microfracture length") and minimum Feret diameter (herein referred to as "pore width" and "microfracture width"). The second type of length and width indicates major axis length of fitting ellipse, minor axis length of fitting ellipse. Geometric parameters include circularity, aspect ratio (ratio of major axis to minor axis of fitting ellipse), solidity and tortuosity [54–56].

Step 4: Construct the intelligent recognition model of pore and microfracture by training above data based on decision tree (DT) method.

Decision tree (DT) is a type of powerful algorithm for data classification. It is represented by a tree structure. Leaf nodes represent classification results, internal nodes describe an attribute. A path from top to bottom determine a classification rule. Compared with other classification methods, DT method has five advantages: (1) DT has strong interpretability, tree structure can be visualized and rules which are easy to understand can be generated; (2) The training needs less data and does not need data normalization. (3) the efficiency is high, and the cost of using DT method is the logarithm of the data points required for training; (4) Able to process continuous and

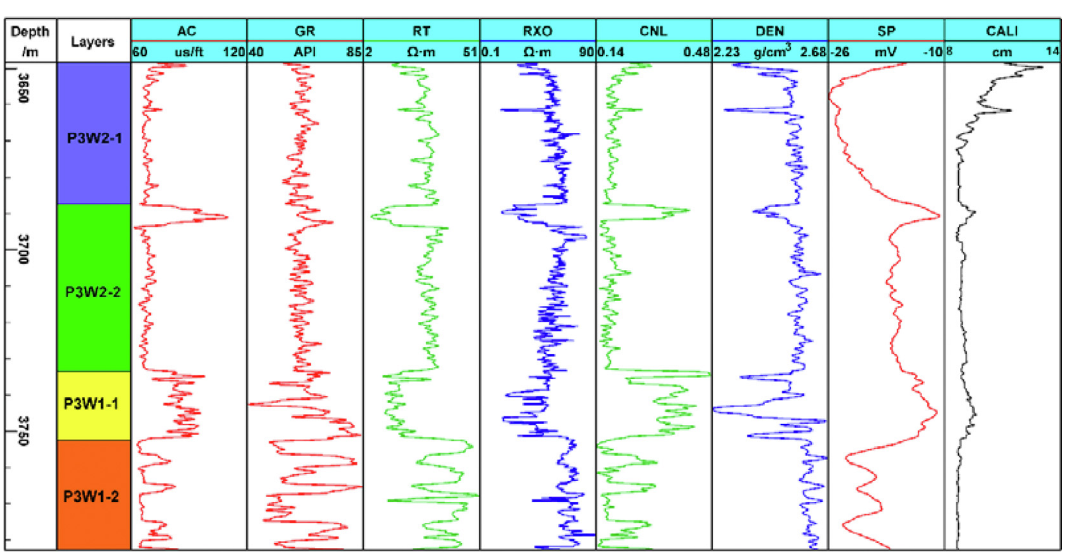

Fig. 1 – The geological horizon division of tight conglomerate reservoir of Upper Wuerhe formation in Mahu 1 well area, Xinjiang (Well name is "K205").

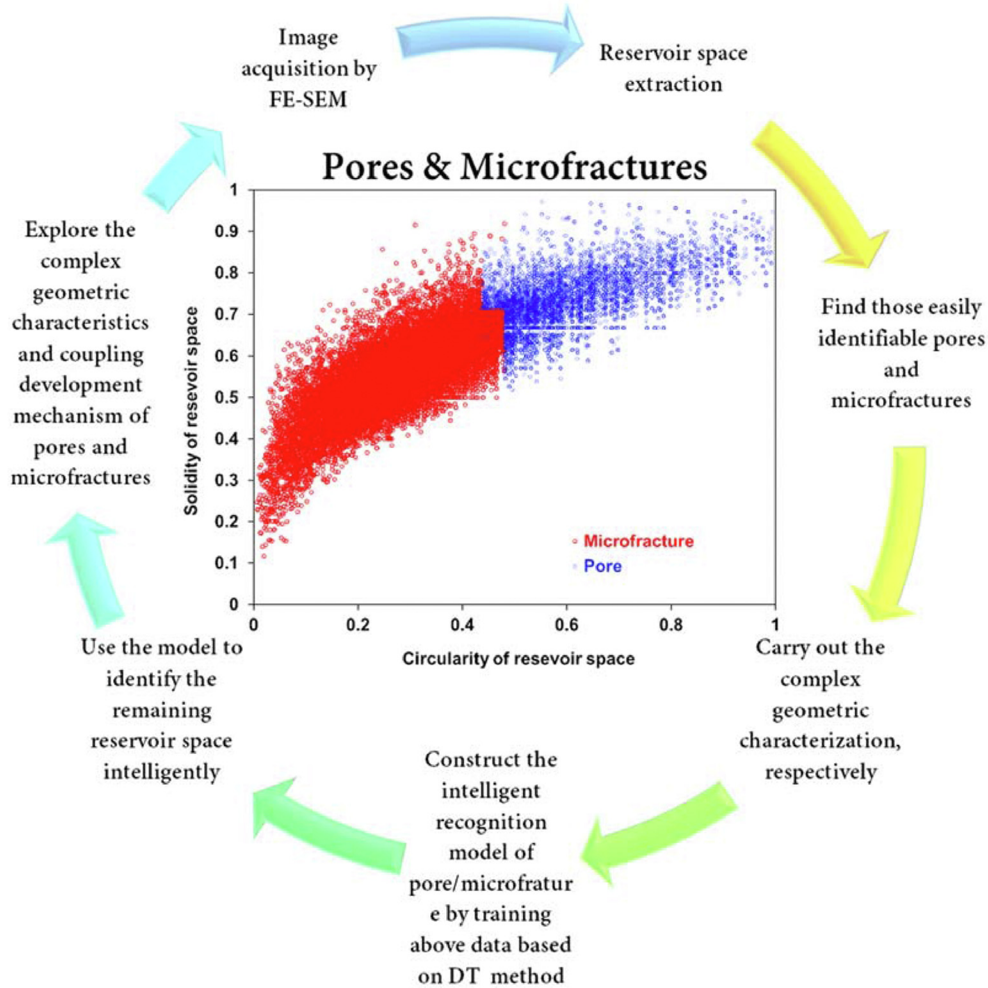

Fig. 2 – The detailed technical routes of this study.

discrete data; (5) Prior knowledge or domain knowledge other than training data is usually not required [57,58].

As we know that the most significant difference between pores and microfractures is nothing more than geometry. In the third step, the shape factor and solidity are optimized as the basis for distinguishing pores and microfractures. Taking the above two types of parameter values of pores and microfractures identified in the second step as independent variables and the attribute characteristics of pores (set to 0) and microfractures (set to 1) as dependent variables, 70% of the data are randomly selected as the training set and the remaining 30% of the data are used as the verification set. Using machine learning [59–61], the intelligent identification model of pores and microfractures could be constructed, and the verification accuracy can be close to 100%.

Step 5: Use the model to identify the remaining reservoir space intelligently. Using the intelligent recognition model established in the fourth step, the complex geometric parameters of the mixed reservoir space of pores and microfractures extracted in the third step are input to complete the purpose of extracting individual pores and microfractures in the remaining reservoir space. The cross-plot figure in the middle of Fig. 2 shows the identified pores and microfractures of Upper Wuerhe reservoir.

Finally, Explore the complex geometric characteristics and coupling development mechanism of pores and microfractures [62–65]. Using correlation trend analysis, the geometric parameters of pores and microfractures are analyzed by multiple intersection to explore the complex development characteristics and mechanism of pores and microfractures.

Results and discussion

The representative recognition results of pores and microfractures

In order to show the geometric characterizations are correctly collected, the characterization results of the size and geometric parameters of typical pores and microfractures are displayed (Fig. 3A–a, 3A-b, and 3A-e, 3A-f), which provides basic data for finding the core parameters to distinguish pores and microfractures via machine learning method.

The typical recognition results of pores and microfractures based on machine learning model are also shown (Fig. 3A–c, 3A-d, and 3A-g, 3A-h). It could prove that the recognition of pores and microfratures based on machine learning method in this study is effective and accurate (Fig. 3).

Geological and engineering significance of pores/microfractures

High resolution imaging based on field emission environmental scanning electron microscope is a necessary and powerful tool for qualitative observation and quantitative analysis of pore and microfracture characteristics. Fig. 4 shows that a large number of residual intergranular pores and secondary corrosion pores are developed in the conglomerate reservoir of each layer of the Upper Wuerhe formation.

It can be qualitatively seen from the electron microscope image that the pore size and tortuosity in the layers of P3W21 and P3W22 (Fig. 4-e, 4-f, 4-g and 4-h) are more homogeneous than which in the layers of P3W11 and P3W22 (Fig. 4-a, 4-b, 4-c and 4-d). However, the connectivity of the above secondary pores is relatively poor, so it is difficult to build a relatively stable seepage system in the actual development process.

Fig. 4 also indicates that microfractures are mainly grain boundary fractures, which constitute the reservoir and seepage space with significant heterogeneity. But the contribution rate still needs to be deeply evaluated. Similarly, compared with the layers of P3W11 and P3W22 (Fig. 4a, b, c and d), the layers of P3W21 and P3W22 have a higher degree of homogeneity in microfracture size and tortuosity (Fig. 4-e, f, g and h). In addition, the microfractures are mostly weak mechanical surface, it is easy to promote the formation of complex fracture network. So it is expected that microfractures will dominate the storage and seepage of hydrocarbon.

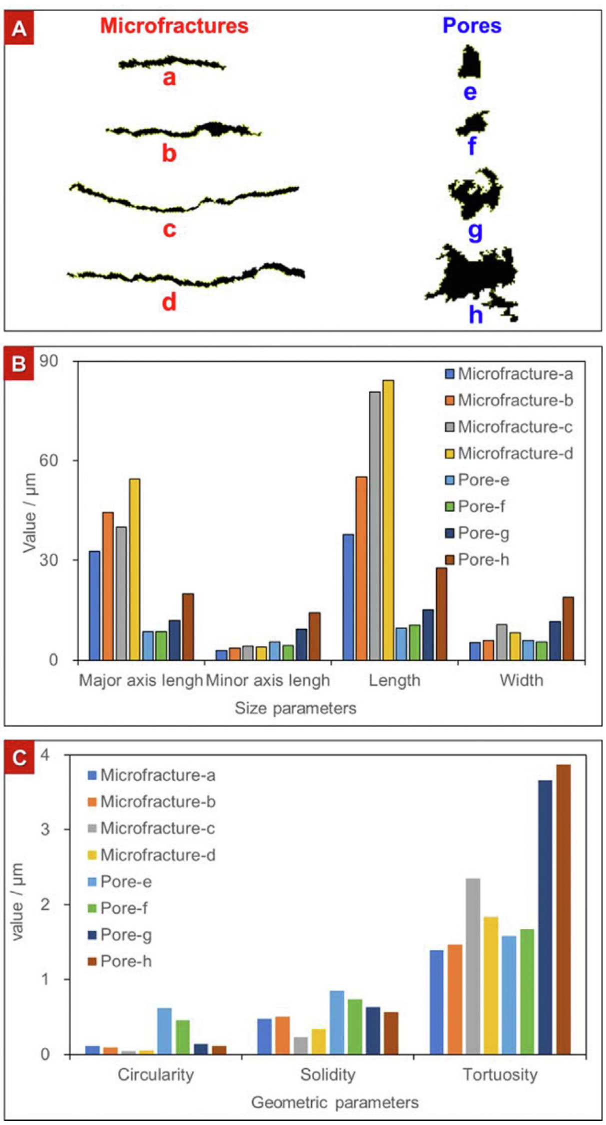

Fig. 3 – Size and geometric characteristics of typical pores and microfractures (A-images of typical microfractures and pores; B- statistics of size parameters; C- statistics of geometric parameters).

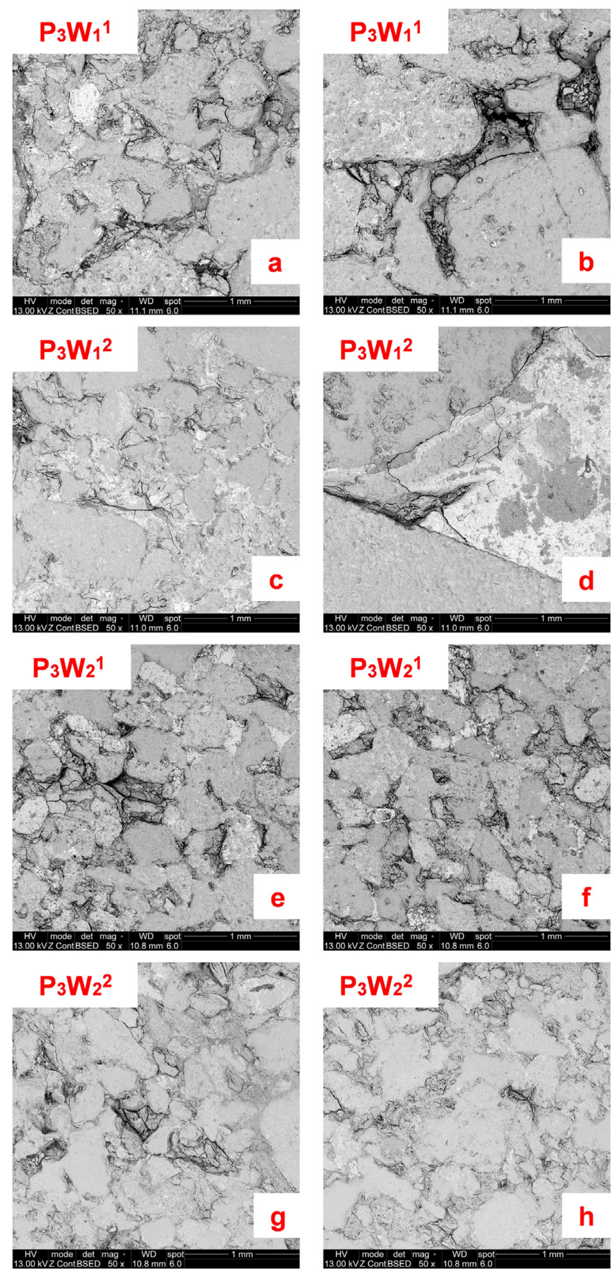

Fig. 4 – SEM images of tight conglomerate of Upper Wuerhe formation.

In order to understand the contribution rate of pores and microfractures to hydrocarbon storage and seepage, we analyze the geological and engineering significance of pores and microfractures in the Upper Wuerhe formation.

Contribution rate of pore/microfractures to reservoir and seepage

Due to the different area proportion of pores and microfractures in the reservoir space, their contribution rates to fluid storage and seepage will be different. For reservoirs with different layers, the contribution rate of pores and microfractures to the storage and seepage of hydrocarbon is heterogeneous (Fig. 5). As for the contribution rate of microfractures to seepage, W21 is the highest (92.75%), and the other three layers have little difference, ranking as W11 (85.92%), W22 (83.97%) and W12 (81.64%) respectively. On the contrary, for the contribution rate of pores to reservoir permeability, W21 is the lowest (7.25%), and there is little difference among the other three layers, ranking W12 (18.36%), W22 (16.03%) and W11 (14.08%) respectively. In addition, the ratio of contribution rate of microfracture and pore to seepage is W21 (12.8), W11 (6.1), W22 (5.2) and W12 (4.4), with an average value of 7.1.

This shows that for the Upper Wuerhe formation, the average contribution rate of microfractures to fluid storage and seepage is 7.1 times that of pores, and microfractures dominate in fluid storage and seepage.

Contact probability between pore/microfracture and fluid

In fact, reservoir damage essentially comes from the dynamic contact between external fluid and porous rock. The seam wall of pore, which is also the mineral surface, is the "direct contact position" between fluid and rock and the "leading edge" of the reservoir damage process. Without the deep participation of external fluid, it is not easy to cause significant reservoir damage. Due to the difference of boundary shape and size between pores and microfractures, the contact probability between oil/water and various pores and microfractures is also different in the process of seepage, which directly affects the difference of pores and microfractures in promoting the degree of reservoir damage. In fact, whether pores or microfractures, the perimeter of their boundaries directly determines the length of the flow path of fluid in the rock. For the same sample, the larger the sum of the perimeter of pores (or microfractures), the higher the probability of contact between pores (or microfractures) and fluid. Therefore, this paper proposes that for a specific conglomerate sample, the sum of the perimeter of all pores (or microfractures) is used to evaluate the contact probability between pores (or microfractures) and fluid in the conglomerate sample, and then further explore the difference between pores and microfractures in promoting the degree of reservoir damage. It should be noted that, the contact probability referred here indicates the contact probability in two dimensional surface, which may deviate from the actual contact probability. In order to narrow the gap between two-dimensional and actual contact probability, then improve the accuracy of the results, for different samples from each layer, we made rock slices from different angles and obtained the average value of the contact probability between rock and fluid in each layer. Therefore, the applicability of the results has been significantly improved.

Similarly, for reservoirs in different geological horizons, the contact probability between pores/microfractures and fluid is also heterogeneous (Fig. 6). The ratio of the contact probability between microfracture/pore and fluid is W21 (4.3), W11 (2.8), W22 (2.5) and W12 (2.2), with an average of 3.0. This shows that for the Upper Wuerhe formation, the average contact probability between microfractures and fluids is three times that of pores.

As can be seen from Figs. 5 and 6, it is obvious that although the average contribution rate of microfractures to fluid storage and seepage is 7 times that of pores, the average contact probability between microfractures and fluids is only 3 times that of pores, not up to 7 times. This shows that the area (volume) ratio of pores/microfractures is not equivalent to their contact probability with fluid. This tells us that for the tight conglomerate reservoir of Upper Wuerhe formation, although microfractures occupy an absolute dominant position in reservoir permeability (The ratio between microfractures and pores equals to 8:1), the role of pores can not be ignored in terms of its contact probability with fluid which is also the probability of

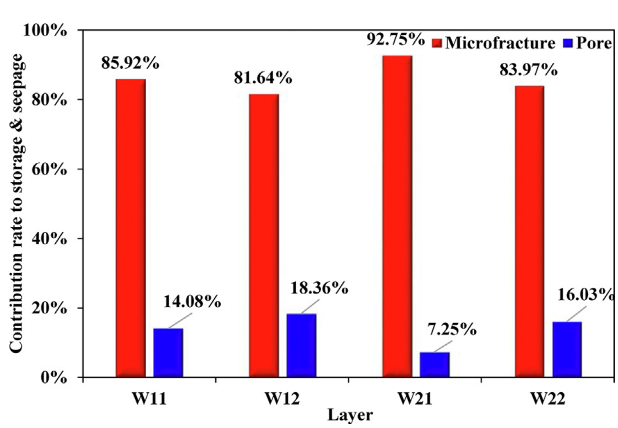

Fig. 5 – The contribution rate of pores/microfractures in four layers of Upper Wuerhe formation to reservoir and seepage.

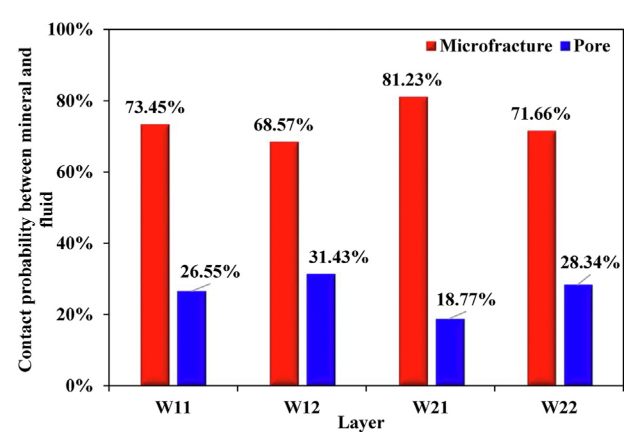

Fig. 6 – Contact probability between pores/microfractures and fluid in four layers of Upper Wuerhe formation.

promoting reservoir damage (the ratio between microfractures and pores equals to 3:1).

Evaluation of homogeneity degree of pore/microfracture size development

Pore radius and microfracture width are two of the most common size parameters affecting fluid storage and permeability. The detailed parameters consist of the radius of all pores and the width of all microfractures in the rock reservoir of each geological horizon, the ratio of the average value of pore radius to the maximum value, the ratio of the average value of fracture width to the maximum value. The above two types of ratios can indicate the homogeneity of the pore radius and microfracture width, respectively.

Fig. 7 shows that W21 is the highest (0.172) in terms of the homogeneity of pore width, and the other three sub layers are W11 (0.151), W22 (0.144) and W12 (0.116) respectively. For the homogeneity of micro crack radius, W22 is the highest (0.047), and the other three layers are W12 (0.031), W21 (0.19) and W11 (0.018) respectively. In addition, the ratio of pore width/microfracture radius homogeneity is W21 (9.2), W11 (8.4), W22 (3.8) and W12 (3.0), with an average of 6.1. This shows that for the Upper Wuerhe formation, the average degree of homogeneity of the pore radius is 6 times that of microfracture width. This shows that compared with microfractures, pores are more conducive to form a homogeneous distribution of seepage flow and expand the sweep efficiency. On the contrary, microfracture is the dominant factor to aggravate the heterogeneity of seepage.

Morphologic homogeneity of pore/microfracture

Similarly, the tortuosity of pores/microfractures is undoubtedly one of the most important geometric parameters to determine the fluid movement path. Based on the traditional definition of tortuosity, in this study, the ratio of half perimeter to the major axis of ellipse is used to represent the tortuosity of pores or microfractures, and then the ratio of the average value of tortuosity to the maximum value is used to evaluate the homogeneity of tortuosity.

Fig. 8 shows that in terms of the homogeneity of pore tortuosity, the overall difference between the four layers is very small, basically distributed between 0.572 and 0.575. For the homogeneity of microfracture tortuosity, W22 is the highest (0.238), and the other three layers are W22 (0.205), W11 (0.177) and W21 (0.139) respectively. In addition, the ratio of pore/microfracture tortuosity to homogeneity is W21 (4.1), W11 (3.2), W22 (2.8) and W12 (2.4), with an average of 3.1. This shows that for the Upper Wuerhe formation, the average degree of homogeneity of pore tortuosity is three times that of microfracture. Similarly, this proves once again that compared with microfractures, pores are more conducive to promote the formation of uniform seepage direction and avoid the formation of water flooding. On the contrary, microfracture is the dominant factor to aggravate the heterogeneity of seepage direction.

It can be seen from the above analysis that, in order to enhance the recovery of hydrocarbon in the area to be exploited, we can carry out high-resolution electron microscope imaging of reservoirs in other research areas. Then we could complete the pores and microfractures identification of all samples by using the intelligent model constructed in this study, and form a new database of pores and microfractures. Besides, we could select the total perimeter and total area of pores and microfractures as the core parameters to evaluate the reservoir damage potential quantitatively, so as to improve the efficiency of exploitation and utilization of hydrocarbon.

Geometric characteristics analysis of pores/microfractures

In terms of the sedimentary and tectonic evolution history of the tight conglomerate of the Upper Wuerhe formation, the formation of multi-scale pores and fractures in the Upper Wuerhe formation has a significant causal relationship with the weathering, denudation, transportation, sedimentation, compaction, and many other geological processes of the parent rock from the provenance area. In other words, the characteristics of pores and microfractures indicate the complexity of geological processes to a great extent. In this study, through the image analysis of above two types of lengths and widths, we can get the development characteristics of pores and microfractures.

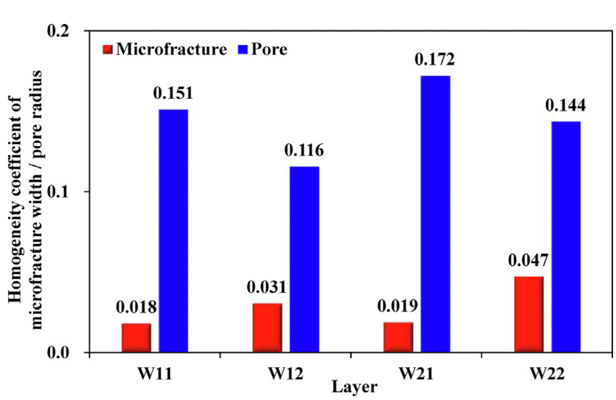

Fig. 7 – Size development homogeneity of pore/microfracture in the four layers of Upper Wuerhe formation.

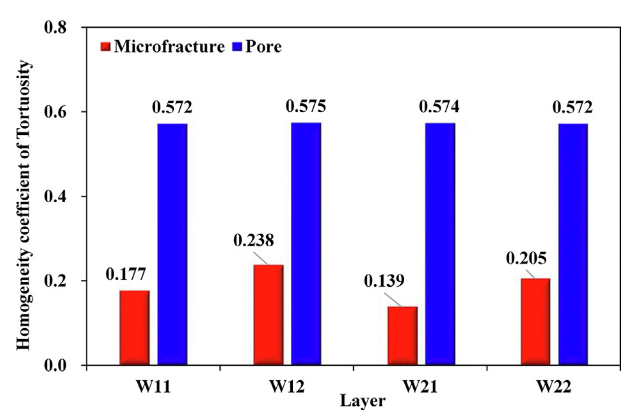

Fig. 8 – Morphological development homogeneity of pore/microfracture in the four layers of Upper Wuerhe formation.

The development of pores and microfractures can be considered to be affected by three main factors: "stress", "cementation", and "corrosion". Generally speaking, the early stage of pore and microfracture development is mainly dominated by compaction and tectonic stress. In the later stage of development, diagenesis process represented by corrosion and cementation gradually participated in the transformation of pores and microfractures, resulting in the gradual complexity of the geometric characteristics of pores and microfractures. The greater the effective stress on pores/microfractures, the higher the reduction of pore/microfracture size. The stronger the corrosion of the mineral boundary constituting pores/microfractures, the worse the cementation, the higher the increase of pore/microfracture size. At the same time, according to the classical geotechnical mechanics theory, when the development of pores/microfractures is dominated by stress, the length and width of microfractures will tend to be linearly correlated, and the higher the correlation coefficient, the more significantly affected by stress. When the pores/microfractures enter the later stage of development, the cementation and corrosion are gradually enhanced. At this time, the size of pores/microfractures is jointly controlled by "stress", "cementation", and "corrosion", its length and width will tend to be non-linear correlation (such as power exponential correlation), and the higher the correlation coefficient, the more significantly affected by corrosion and cementation. According to the above basic understanding, the development mechanism of pores and microfractures in Upper Wuerhe formation are analyzed below.

As for the layer of W11, the correlation between length and width in microfractures is slightly higher than that in pores. It may indicate that the degree of corrosion and cementation effect in pores is slightly higher than which in microfractures (Fig. 9). Reservoir cementation degree in pores of W11 is high, and the grain boundary fractures and pores are relatively developed (Fig. 10).

As for the layer of W12, the correlation between length and width in pores is slightly higher than that in microfractures. It may indicate that the degree of corrosion and cementation effect in microfractures is slightly higher than which in pores (Fig. 9). Reservoir cementation degree in microfractures of W12 is higher than which in the other three layers, and the grain boundary fractures and pores are relatively developed (Fig. 10).

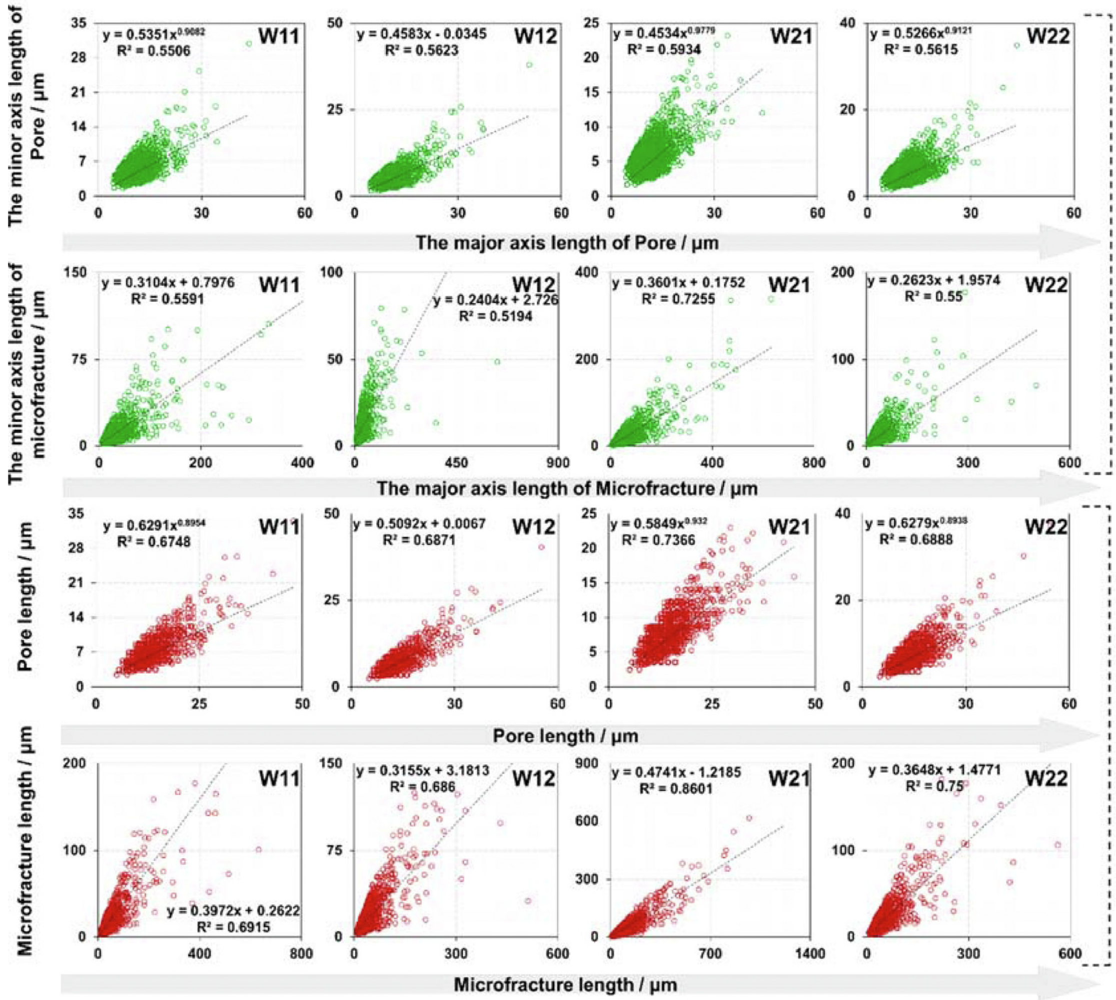

Fig. 9 – Correlation analysis of two groups of length parameters of pores/microfractures in W11, W12, W21 and W22 member of Upper Wuerhe formation.

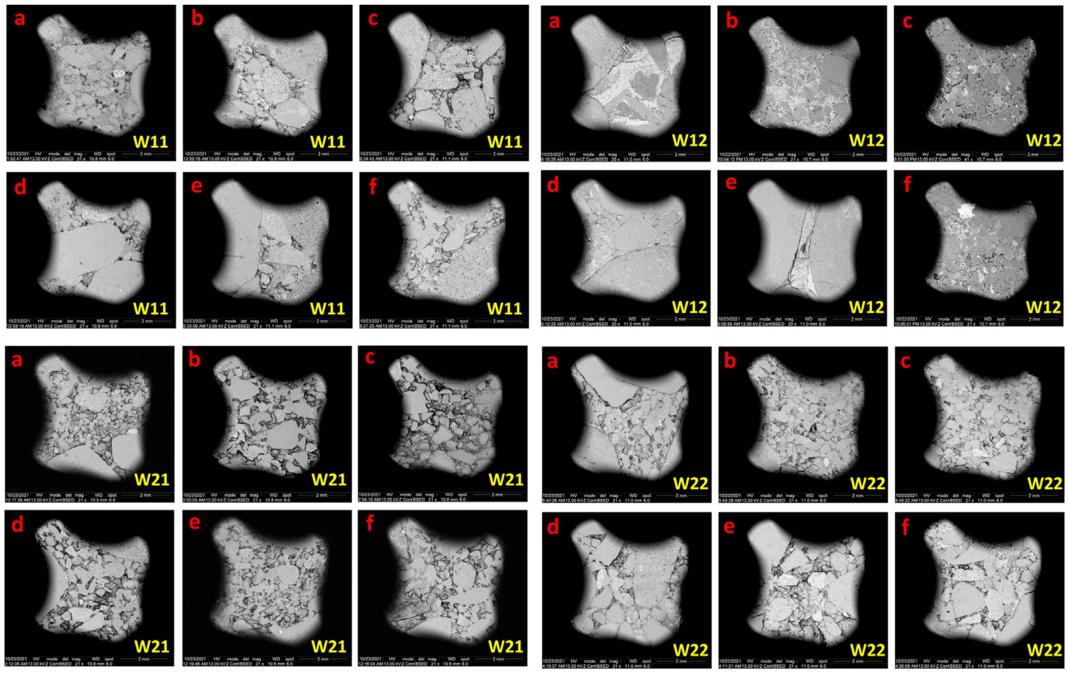

Fig. 10 – SEM images of pores/microfractures in W11, W12, W21 and W22 member of Upper Wuerhe formation.

Overall, as for the layer of W21 and W22, the correlation between length and width in microfractures is apparently higher than that in pores. It may indicate that the degree of corrosion and cementation effect in pores is significantly higher than which in microfractures (Fig. 9). Reservoir cementation degrees in pores of W21 and W22 are high but relatively low in microfractures (Fig. 10).

We summarize the data of the four layers in 3.2 (Fig. 11 and Table 1). Table 1 shows that for the Upper Wuerhe formation, the pore development is jointly affected by stress and corrosion, while the microfracture development is mainly dominated by stress. For the four layers, there is significant heterogeneity among them. As to the layer of W12, the square of the correlation coefficient between the major axis length and minor axis length of microfractures (0.5194) does not mean poor correlation since it is based on the statistical analysis of 18,132 microfractures. So it can still indicate that there is a significant positive correlation between the major axis length and minor axis length of microfractures for W12 layer.

It should be noted that for reservoirs at different horizons, the square of correlation coefficient "R^2" between pore length (or major axis length) and width (or minor axis length) have passed the statistical significance test (Figs. 9 and 11 and Table 1), which is fit to the change law of pore morphology during reservoir deposition and compaction.

There is no doubt that the correlation coefficient between pore length (or minor axis length) and width (or minor axis length) can be improved when the original mineral particles forming the reservoir have good sorting degree and the geological process is uniform in the critical period of rock formation.

The coupling development mechanism between pore and microfracture

As we know, pores and microfractures co-exist in rocks, their development must be closely related. This coupling development mechanism is worthy of further exploration.

Therefore, we analyze the complex geometric characteristics of pores and microfractures, and try to find the internal relationship between pores and microfractures in size and shape development.

The orientation of pores and microfractures directly affects the anisotropy of seepage direction, and then determines the final mining effect. Based on the advantage of standard deviation in characterizing the degree of data dispersion, we calculated the standard deviation of pore/microfracture extension angle in each field of view. The smaller the standard deviation, the better the orientation of pores and microfractures.

The heterogeneity of pore aspect ratio can be expressed by the standard deviation of pore aspect ratio. The larger the standard deviation, the higher the degree of heterogeneity. Fig. 12-a shows that the greater the heterogeneity of microfracture extension angle, that is, the worse the orientation of microfracture, the stronger the heterogeneity of pore aspect ratio.

Fig. 12-b shows that the stronger the heterogeneity of microfracture aspect ratio, the weaker the heterogeneity of pore tortuosity. This shows that there is a reverse promoting relationship between the heterogeneity of aspect ratio of microfractures and the heterogeneity of pore tortuosity.

Fig. 12-c and 12-h show that the tortuosity and orientation of pores and microfractures show a positive correlation trend, which shows that the tortuosity and orientation of pores and

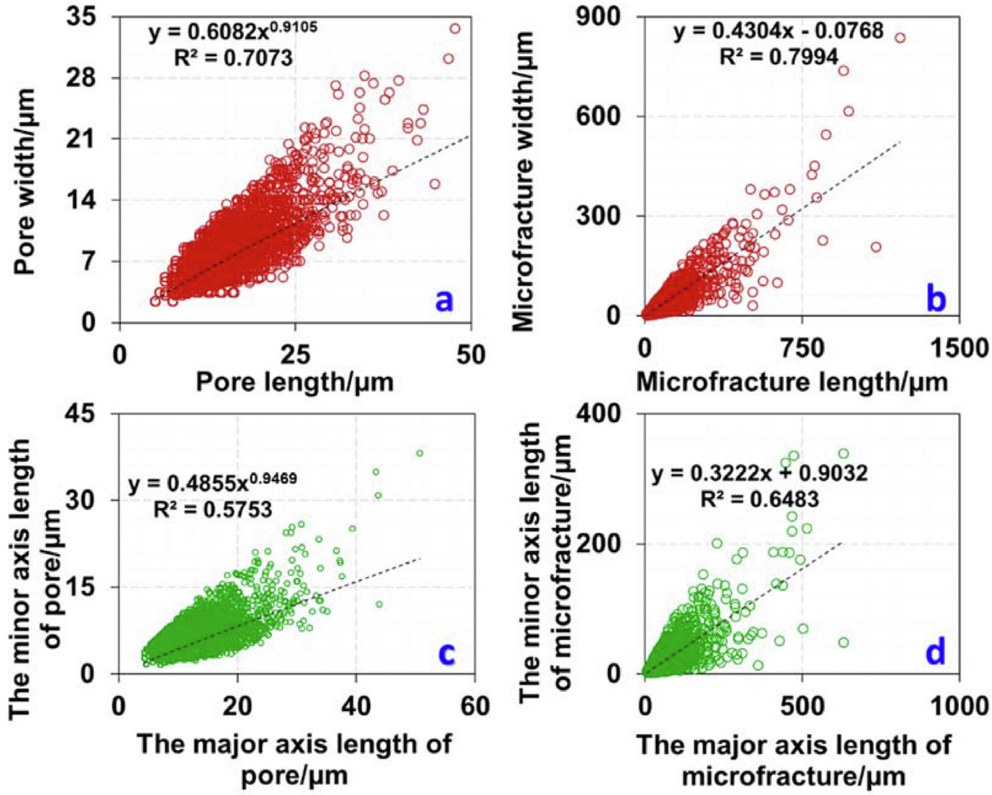

Fig. 11 – **Correlation analysis of two groups of length parameters of pores/microfractures in the Upper Wuerhe formation.**

microfractures change in the same direction with the progress of a series of geological processes such as sedimentation, structure and diagenesis.

Fig. 12-d shows that the smaller the microfracture shape factor, the higher the probability of contact with the fluid. This shows that the more the shape of microfractures deviates from the circle, the more conducive it is to the spread of fluid.

Fig. 12-e, 12-f, 12-g and 12-i show that the larger the microfracture opening, the lower the pore aspect ratio, the lower the ovality, the higher the roundness and the higher the tortuosity. This shows that there is a reverse promoting relationship between the opening of microfracture and the change of pore aspect ratio. For conglomerate, when the average opening of microfractures is large, the roundness and tortuosity of pores are also high.

In general, the heterogeneous extension angle of microfracture is easy to lead to heterogeneous aspect ratio of pore, while heterogeneous aspect ratio of microfracture is easy to lead to relatively homogeneous tortuosity of pore. It can prove that the development of microfractures and pores in size and shape has an interactive process, and the control mechanism is extremely complex (Fig. 12).

Table 1 – **Statistics of correlation analysis results of two groups of length parameters of pores/microfractures in Upper Wuerhe formation.**

Complex geometric	Layers	R square		Fitting function type	
		Pore	Microfracture	Pore	Microfracture
Feret diameter(Length) & MinFeret diameter (Width)	Total	0.7073	0.7994	power	Linear
	w11	0.6748	0.6915	power	Linear
	w12	0.6871	0.6860	Linear	Linear
	w21	0.7366	0.8601	power	Linear
	w22	0.6888	0.7500	power	Linear
Major axis length & Minor axis length	Total	0.5753	0.6483	power	Linear
	w11	0.5506	0.5591	power	Linear
	w12	0.5623	0.5194	Linear	Linear
	w21	0.5934	0.7255	power	Linear
	w22	0.5615	0.5500	power	Linear

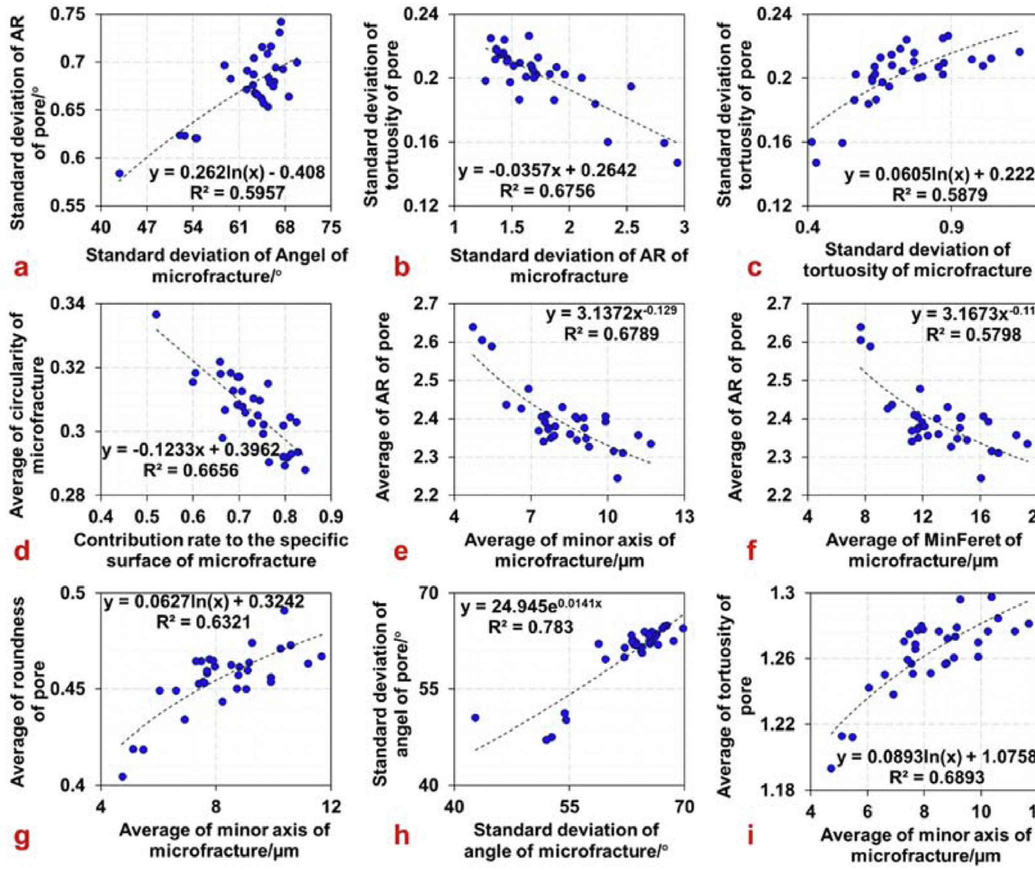

Fig. 12 – Analysis of coupling development mechanism of pores/microfractures in Upper Wuerhe formation.

Conclusion

It is concluded that for of the tight conglomerate reservoir of the Upper Wuerhe formation in Xinjiang of China, the contribution rate of pore/microfracture to reservoir and seepage, the contact probability between pore/microfracture and fluid are heterogeneous in four layers include W11, W12, W21 and W22. Compared with microfractures, pores are more conducive to promote the formation of uniform seepage direction and avoid the formation of water flooding. On the contrary, microfractures are the dominant factor to aggravate the heterogeneity of seepage process.

The development of microfractures and pores in size and shape has an interactive process. For W21, W22 and W11, the degree of corrosion and cementation effect in pores is higher than which in microfractures which is opposite to which in W12. The heterogeneous extension angle of microfracture is easy to lead to heterogeneous aspect ratio of pore, while heterogeneous aspect ratio of microfracture is easy to lead to relatively homogeneous tortuosity of pore.

Finally, the exact geological significance of many geometric parameters in this paper still needs to be tested or even corrected in many future studies and practices.

Declaration of competing interest

The authors declare that they have no known competing financial interests or personal relationships that could have appeared to influence the work reported in this paper.

Acknowledgements

This work was jointly supported by National Natural Science Foundation of China (NSFC, Grant No. 41902132, 12032019, 11872363). Thanks for the crucial recognitions of editors and anonymous reviewers.

REFERENCES

[1] Li J, Yang Z, Wu S, Pan S. Key issues and development direction of petroleum geology research on source rock strata in China. Adv Geo-Energy Res 2021;5(2):121–6. https://doi.org/10.46690/ager.2021.02.02.

[2] Nikolenko PV, Epshtein SA, Shkuratnik VL, Anufrenkova PS. Experimental study of coal fracture dynamics under the

influence of cyclic freezing–thawing using shear elastic waves. Int J Coal Sci Technol 2021;8(4):562–74. https://doi.org/10.1007/s40789-020-00352-x.
[3] Liu X, Wei L, Liu B, Zhang L, Guo W, Zhang J, Zheng J. Characteristics of natural gas accumulation in the Cambrian weathered crust in southwestern Ordos Basin. Nat Gas Ind B 2021;8(5):421–30. https://doi.org/10.1016/j.ngib.2021.08.001.
[4] Keboletse KP, Ntuli F, Oladijo OP. Influence of coal properties on coal conversion processes-coal carbonization, carbon fiber production, gasification and liquefaction technologies: a review. Int J Coal Sci Technol 2021;8(5):817–43. https://doi.org/10.1007/s40789-020-00401-5.
[5] Su DWH, Zhang P, Dougherty H, Van Dyke M, Kimutis R. Longwall mining, shale gas production, and underground miner safety and health. Int J Min Sci Technol 2021;31(3):523–9. https://doi.org/10.1016/j.ijmst.2020.12.013.
[6] Liu PG, Du SH, Hou F. Quantitative characterization of fracturing effect of tight reservoir based on full-length fracturing simulation technology. J China Univ Petrol Edition of Nat Sci 2020;44(5):10–8. https://doi.org/10.3969/j.issn.1673-5005.2020.05.002.
[7] Gao SC, Ren ZJ. Adsorption property of shale gas based on Monte-Carlo method. Chin J Appl Mech 2020;(3):1314–20. https://doi.org/10.11776/cjam.37.03.D013.
[8] Ji L, Liu YM, Guo XL, Wang F, Zhang RJ, Sun J, et al. Geological controlling factors of single well productivity in perforated and fractured reservoir in Zaoyuan oilfield. Petrol Sci Bullet 2021;4:566–75. https://doi.org/10.3969/j.issn.2096-1693.2021.04.039.
[9] Li CX, Liu DD, Xiao L, Jang ZX, Li Z, Guo J. Research into pore evolution in Cretaceous continental shales in the Songliao Basin. Petrol Sci Bullet 2021;2:181–95. https://doi.org/10.3969/j.issn.2096-1693.2021.02.015.
[10] Wei SS, Shen JS, Li ZL, Di SH, Yang WY, Yan GL. Calculation of effective permeability based on approximation of 3D renormalization. J China Univ Petrol Edition of Nat Sci 2020;44(1):34–44. https://doi.org/10.3969/j.issn.1673-5005.2020.01.004.
[11] Zhao XJ, Qu Z, Fan H, Wang P, An FJ. Calculation model of shale fracturing pressure based on seepage and hydration. Chin J Appl Mech 2019;(2):249–53. https://doi.org/10.11776/cjam.36.02.B007.
[12] Sun S, Zhao SX, Hou JG, Zhou YB, Song SH, He YF. Hierarchical modeling of multi-scale fractures in tight sandstones: a case study of the eighth member of the Yanchang formation in wellblock 92 of the Honghe oilfield. Petrol Sci Bullet 2019;1:11–26. https://doi.org/10.3969/j.issn.2096-1693.2019.01.002.
[13] Liu XF, Zhang XW, Zeng Xin, Cheng DJ, Ni H, Li CL, et al. Pore structure characterization of shales using SEM and machine learningbased segmentation method. J China Univ Petrol Edition of Nat Sci 2022;46(1):23–33. https://doi.org/10.3969/j.issn.1673-5005.2022.01.003.
[14] Han Q, Qu Z, Ye ZY. Research status of shale multi-scale mechanical properties. Chin J Appl Mech 2018;(3):564–70. https://doi.org/10.11776/cjam.35.03.B119.
[15] Wang JJ, Wu SH, Xiao SM, Guo QH, Lü ZQ, Jiao HY, et al. Distribution characteristics of micro pore throat size of turbidite sandstone reservoir in middle sub-rnember of 3rd member, Shahejie Formation in Dongying Depression. J China Univ Petrol Edition of Nat Sci 2021;45(4):12–21. https://doi.org/10.3969/j.issn.1673-5005.2021.04.002.
[16] Teng XQ, Chen M, Jin Y, Lu YH, Xia Y. Poroelastic dynamics mechanisms of wellbore instability in tight formations. Petrol Sci Bullet 2017;4:478–89. https://doi.org/10.3969/j.issn.2096-1693.2017.04.044.
[17] Xiao X, Lan Y, Chen J. Learning from nature for healthcare, energy, and environment. Innovation 2021;2(3):100135. https://doi.org/10.1016/j.xinn.2021.100135.
[18] Li TW, Jiang ZX, Xu CL, Zhu RF, Li X, Chen WT, et al. Shale micro–nano pore structure characteristics in the lower third member of the continental Shahejie Formation, Zhanhua Sag. Petrol Sci Bullet 2017;4:445–56. https://doi.org/10.3969/j.issn.2096-1693.2017.04.041.
[19] Cheng H. Future earth and sustainable developments. Innovation 2020;1(3):100055. https://doi.org/10.1016/j.xinn.2020.100055.
[20] Wu KL, Chen ZX. Review of gas transport in nanopores in shale gas reservoirs. Petrol Sci Bullet 2016;1:91–127. https://doi.org/10.3969/j.issn.2096-1693.2016.01.007.
[21] Chen JM. Carbon neutrality: toward a sustainable future. Innovation 2021;2(3):100127. https://doi.org/10.1016/j.xinn.2021.100127.
[22] Cai L, Xiao G, Lu S, Wang J, Wu Z. Spatial-temporal coupling between high-quality source rocks and reservoirs for tight sandstone tight conglomerate accumulations in the Songliao Basin, China. Int J Min Sci Technol 2019;29(3):387–97. https://doi.org/10.1016/j.ijmst.2019.03.006.
[23] Xu G, Yin H, Yuan H, Xing C. Decline curve analysis for multiple-fractured horizontal wells in tight tight conglomerate reservoirs. Advances in Geo-Energy Research 2020;4(3):296–304. https://doi.org/10.46690/ager.2020.03.07.
[24] Li GX, Qin JH, Xian CG, Fan XB, Zhang J, Ding Y. Theoretical understandings, key technologies and practices of tight conglomerate field efficient development: a case study of the Mahu tight conglomerate field, Junggar Basin, NW China. Petrol Explor Dev 2020;47(6):1275–90. https://doi.org/10.1016/S1876-3804(20)60135-0.
[25] Li J, Tang Y, Wu T, Zhao JZ, Wu HY, Wu WT. Overpressure origin and its effects on petroleum accumulation in the conglomerate tight conglomerate province in Mahu Sag, Junggar Basin, NW China. Petrol Explor Dev 2020;47(4):726–39. https://doi.org/10.1016/S1876-3804(20)60088-X.
[26] Xi K, Cao Y, Haile BG, Zhu N, Liu K, Wu S, Hellevang H. Diagenetic variations with respect to sediment composition and paleo-fluids evolution in conglomerate reservoirs: a case study of the Triassic Baikouquan Formation in Mahu Sag, Junggar Basin, Northwestern China. J Petrol Sci Eng 2021;197:107943. https://doi.org/10.1016/j.petrol.2020.107943.
[27] Zou YS, Shi SZ, Zhang SC, Yu TX, Tian G, Ma XF, et al. Experimental modeling of sanding fracturing and conductivity of propped fractures in conglomerate: a case study of tight conglomerate of Mahu sag in Junggar Basin, NW China. Petrol Explor Dev 2021;48(6):1383–92. https://doi.org/10.1016/S1876-3804(21)60294-X.
[28] Cheng F, Li Y, Wang M, Pang H, Chen X, Lv Z. Fracturing optimization of new wells considering cross-well interference in the Mahu conglomerate reservoir. Chem Technol Fuels Tight conglomerates 2022;57(6):1022–9. https://doi.org/10.1007/s10553-022-01339-x.
[29] Yang K, Zhou D, Yang B, Tong J, Luo S, Chen Y, et al. The depositional evolution and controlling factors of the lower triassic baikouquan formation, northern Mahu slope, Junggar Basin, NW China. Geol J 2021;56(5):2720–35. https://doi.org/10.1002/gj.4064.
[30] Zhou Y, Wu S, Li Z, Zhu R, Xie S, Jing C, et al. Multifractal study of three-dimensional pore structure of sand-conglomerate reservoir based on CT Images. Energy Fuels

2018;32(4):4797–807. https://doi.org/10.1021/acs.energyfuels.8b00057.

[31] Chen H, Lv Q, Gao J, Yu J, Pang Y, Li B, et al. The characteristics and controlling factors of glutenite reservoirs in the permian upper urho formation, southern zhongguai rise, Junggar Basin, NW China. Geol J 2022;57(1):221–37. https://doi.org/10.1002/gj.4293.

[32] Wang L, Zhao N, Sima L, Meng F, Guo Y. Pore structure characterization of the tight reservoir: systematic integration of mercury injection and nuclear magnetic resonance. Energy Fuels 2018;32(7):7471–84. https://doi.org/10.1021/acs.energyfuels.8b01369.

[33] Wang S, Wang G, Huang L, Song L, Zhang Y, Li D, et al. Logging evaluation of lamina structure and reservoir quality in shale tight conglomerate reservoir of Fengcheng Formation in Mahu Sag, China. Mar Petrol Geol 2021;133:105299. https://doi.org/10.1016/j.marpetgeo.2021.105299.

[34] Zhang G, Wang Z, Guo X, Sun Y, Sun L, Pan L. Characteristics of lacustrine dolomitic rock reservoir and accumulation of tight tight conglomerate in the Permian Fengcheng Formation, the western slope of the Mahu Sag, Junggar Basin, NW China. J Asian Earth Sci 2019;178:64–80. https://doi.org/10.1016/j.jseaes.2019.01.002.

[35] Guo J, Huang Y, Wang Y, Pan J, Huang L. Quality evaluation of glutenite reservoirs of intergranular-Secondary corrosion pore type using a quantitative method. Energy Geoscience 2022;3(2):126–33. https://doi.org/10.1016/j.engeos.2022.01.003.

[36] Xiao M, Yuan X, Cheng D, Wu S, Cao Z, Tang Y, et al. Feldspar corrosion and its influence on reservoirs: a case study of the Lower Triassic Baikouquan Formation in the northwest margin of the Junggar Basin, China. Geofluids 2018:6536419. https://doi.org/10.1155/2018/6536419.

[37] Abitkazy T, Du S, Xu F, Shi Y. Pore structure characterization of clay minerals in the lower karamay formation conglomerate reservoir in the Junggar Basin and its impact on hydrocarbon storage and seepage. Acta Geologica Sinica-English Edition 2021;95(2):558–69. https://doi.org/10.1111/1755-6724.13887.

[38] Shi X, Qin Y, Xu H, Feng Q, Wang S, Xu P, Han S. Numerical simulation of hydraulic fracture propagation in conglomerate reservoirs. Eng Fract Mech 2021;248:107738. https://doi.org/10.1016/j.engfracmech.2021.107738.

[39] Nie RS, Zhou J, Chen Z, Liu J, Pan Y. Pore structure characterization of tight sandstones via a novel integrated method: a case study of the Sulige gas field, Ordos Basin (Northern China). J Asian Earth Sci 2021;213:104739. https://doi.org/10.1016/j.jseaes.2021.104739.

[40] Li S, Han R, Du Y, Liu P, Bie H. Quantitative characterization of diagenetic reservoir facies of the Karamay alluvial fan in the Junggar Basin, western China. J Petrol Sci Eng 2020;188:106921. https://doi.org/10.1016/j.petrol.2020.106921.

[41] Liu G, Chen Z, Wang X, Gao G, Xiang B, Ren J, et al. Migration and accumulation of crude tight conglomerates from Permian lacustrine source rocks to Triassic reservoirs in the Mahu depression of Junggar Basin, NW China: constraints from pyrrolic nitrogen compounds and fluid inclusion analysis. Org Geochem 2016;101:82–98. https://doi.org/10.1016/j.orggeochem.2016.08.013.

[42] Zhou L, Zhou K, Wang G. Distribution features and main controlling factors of volcanic buried hill reservoirs in carboniferous basement of Junggar Basin. Arabian J Geosci 2020;13(24):1–11. https://doi.org/10.1007/s12517-020-06319-1.

[43] Wang J, Ge H, Liu J, Shen Y, Zhang Z, Luo S, et al. Effects of gravel size and content on the mechanical properties of conglomerate. Rock Mech Rock Eng 2022;55:2493–502. https://doi.org/10.1007/s00603-021-02760-0.

[44] Sheng G, Su Y, Zhao H, Liu J. A unified apparent porosity/permeability model of organic porous media: coupling complex pore structure and multi-migration mechanism. Advances in Geo-Energy Research 2020;4(2):115–25. https://doi.org/10.26804/ager.2020.02.01.

[45] Tian X, He X, Song D, Li Z, Khan M, Liu H, et al. AFM characterization of surface mechanical and electrical properties of some common rocks. Int J Min Sci Technol 2021;32(2):435–45. https://doi.org/10.1016/j.ijmst.2021.12.008.

[46] Zhang L, Mo J, Cheng X, Zhang S. Evaluation of ceramsite loss control agent in acid fracturing of naturally fractured carbonate reservoir. Nat Gas Ind B 2021;8(3):302–8. https://doi.org/10.1016/j.ngib.2021.04.007.

[47] Liu Y. Field tests of high-density tight conglomerate-based drilling fluid application in horizontal segment. Nat Gas Ind B 2021;8(3):231–8. https://doi.org/10.1016/j.ngib.2021.04.003.

[48] Liu C, Zhang L, Li Y, Liu F, Martyushev DA, et al. Effects of microfractures on permeability in carbonate rocks based on digital core technology. Advances in Geo-Energy Research 2022;6(1):86–90. https://doi.org/10.46690/ager.2022.01.07.

[49] Xue D, Zhang Z, Chen C, Zhou J, Lu L, Sun X, et al. Spatial correlation-based characterization of acoustic emission signal-cloud in a granite sample by a cube clustering approach. Int J Min Sci Technol 2021;31(4):535–51. https://doi.org/10.1016/j.ijmst.2021.05.008.

[50] He X, He G, Gao Y, Zhang P, Lu S, Wan J. Geological characteristics and enrichment laws of normal-pressure shale gas in the basin-margin transition zone of SE Chongqing. Nat Gas Ind B 2019;6(4):333–46. https://doi.org/10.3787/j.issn.1000-0976.2018.12.001.

[51] Ye D, Liu G, Gao F, Xu R, Yue F. A multi-field coupling model of gas flow in fractured coal seam. Advances in Geo-Energy Research 2021;5(1):104–18. https://doi.org/10.46690/ager.2021.01.10.

[52] Kang Y, Rao Q, Zhao Q, Wang H. Exploration and development potential of the low-maturity continental shale gas in the Fuxin Basin. Nat Gas Ind B 2019;6(5):435–43. https://doi.org/10.1016/j.ngib.2019.03.002.

[53] Wang Z, Qin Y, Li T, Zhang X. A numerical investigation of gas flow behavior in two-layered coal seams considering interlayer interference and heterogeneity. Int J Min Sci Technol 2021;31(4):699–716. https://doi.org/10.1016/j.ijmst.2021.05.003.

[54] Du SH. Characteristics and the formation mechanism of the heterogeneous microfractures in the tight oil reservoir of Ordos Basin, China. J Petrol Sci Eng 2020;191:107176. https://doi.org/10.1016/j.petrol.2020.107176.

[55] Shi GX, Kou G, Du SH, Wei Y, Zhou W, Zhou B, et al. What role would the pores related to brittle minerals play in the process of oil migration and oil & water two-phase imbibition? Energy Rep 2020;6:1213–23. https://doi.org/10.1016/j.egyr.2020.04.031.

[56] Zeng YJ, Du SH, Zhang X, Zhang BP, Liu HL. The crucial geometric distinctions of microfractures as the indispensable transportation channels in hydrocarbon-rich shale reservoir. Energy Rep 2020;6:2056–65. https://doi.org/10.1016/j.egyr.2020.07.004.

[57] Baysal M, Günay ME, Yıldırım R. Decision tree analysis of past publications on catalytic steam reforming to develop heuristics for high performance: a statistical review. Int J Hydrogen Energy 2017;42(1):243–54. https://doi.org/10.1016/j.ijhydene.2016.10.003.

[58] Rahnama A, Zepon G, Sridhar S. Machine learning based prediction of metal hydrides for hydrogen storage, part I:

prediction of hydrogen weight percent. Int J Hydrogen Energy 2019;44(14):7337–44. https://doi.org/10.1016/j.ijhydene.2019.01.261.
[59] İskenderoğlu FC, Baltacioğlu MK, Demir MH, Baldinelli A, Barelli L, Bidini G. Comparison of support vector regression and random forest algorithms for estimating the SOFC output voltage by considering hydrogen flow rates. Int J Hydrogen Energy 2020;45(60):35023–38. https://doi.org/10.1016/j.ijhydene.2020.07.265.
[60] Suwarno S, Dicky G, Suyuthi A, Effendi M, Witantyo W, Noerochi L, et al. Machine learning analysis of alloying element effects on hydrogen storage properties of AB2 metal hydrides. Int J Hydrogen Energy 2022;47(23):11938–47. https://doi.org/10.1016/j.ijhydene.2022.01.210.
[61] Saadetnejad D, Oral B, Can E, Yıldırım R. Machine learning analysis of gas phase photocatalytic CO_2 reduction for hydrogen production. Int J Hydrogen Energy 2020;47(45):19655–68. https://doi.org/10.1016/j.ijhydene.2022.02.030.
[62] Du SH, Shi YM. Rapid determination of complete distribution of pore and throat in tight oil sandstone of Triassic Yanchang Formation in Ordos Basin, China. Acta Geol Sin-Engl 2020;94(3):822–30. https://doi.org/10.1111/1755-6724.13881.
[63] Du SH, Shi YM, Guan P. Fluid filling rule in intra-granular pores of feldspar and fractal characteristics: a case study on Yanchang Formation tight sandstone reservoir in Ordos Basin. Earth Sci 2019;44(12):4252–63. https://doi.org/10.3799/dqkx.2018.199.
[64] Du SH. Anisotropic rock poroelasticity evolution in ultra-low permeability sandstones under pore pressure, confining pressure, and temperature: experiments with biot's coefficient. Acta Geol Sin-Engl 2021;95(3):937–45. https://doi.org/10.1111/1755-6724.13886.
[65] Du SH, Pang S, Chai GS, Wang H, Shi YM. Quantitative analysis on the microscopic anisotropy characteristics of pore and mineral in tight reservoir by "Umbrella Deconstruction" method. Earth Sci 2020;45(1):276–84. https://doi.org/10.3799/dqkx.2018.567.